



## Performance Analysis of a Novel Cross-flow Solar Air Heater with Square Perforated Absorber Plate: An Experimental Study

H. Farzan<sup>1\*</sup>, A. A. Abouee-Mehrizi<sup>2</sup>, M. Khazali<sup>3</sup>

<sup>1</sup> Mechanical Engineering Department, Faculty of Engineering, Higher Education Complex of Bam, Bam, Iran

<sup>2</sup> Industrial Engineering Department, Faculty of Engineering, Higher Education Complex of Bam, Bam, Iran

<sup>3</sup> Mathematics Department, Faculty of Mathematics and Computing, Higher Education Complex of Bam, Bam, Iran

### PAPER INFO

#### Paper history:

Received 17 April 2023

Accepted in revised form 10 May 2023

#### Keywords:

Cross-flow perforated solar air heaters

Perforations

Thermal efficiency

Transient dynamics

### ABSTRACT

The current study introduces and analyzes a novel square cross-flow perforated solar air heater (SAH). Since the convection mechanism in SAHs is weak, numerous methods have been suggested to address this problem and improve thermal efficiency. Perforations and cross-flow configuration generate high turbulence and, consequently, high convection rate resulted. Hence these methods have been applied to enhance thermal efficiency. To achieve this goal, an experimental setup was fabricated and tested at outdoor conditions for two air mass flow rates ( $m_{air}$ ) of 0.015 kg/s and 0.03 kg/s while several sensors monitored the collector's heat dynamics and ambient conditions. The obtained results illustrate that outlet temperature reaches the peak values of 38 °C and 34 °C, which is only 6 °C and 7 °C lower than the maximum absorber temperature. This crucial issue proves a high heat exchange rate in the fabricated SAH that causes the absorber temperature to approach the outlet temperature due to high turbulence. The strong convection mechanism in the fabricated SAH improves daily thermal efficiency, in which its value reaches nearly 78.6% for the mass flow rate of 0.03 kg/s. In conclusion, the square cross-flow perforated SAH is an economy, applicable, compact collector, ensuring high thermal efficiency.

doi: 10.5829/ijee.2023.14.04.08

### NOMENCLATURE

$A_c$	Collector surface area (m <sup>2</sup> )	$w$	Uncertainty
$c_p$	Specific heat capacity (J/kg.K)	<b>Subscript</b>	
$G$	Solar intensity (W/m <sup>2</sup> )	$in$	Inlet
$\dot{m}$	Mass flow rate (kg/s)	$out$	Outlet
$Q$	Harnessed gain (J)	<b>Greek Symbols</b>	
$T$	Temperature (°C)	$\eta_{1,Daily}$	Daily thermal efficiency

### INTRODUCTION

Global warming urges many politicians to utilize renewable energy sources to meet residential and industrial requirements. Since incoming solar energy is the most abundant, reliable renewable energy source, numerous methods were suggested to extract this energy

source [1]. Solar air heaters (SAHs) are a simple, cheap technique widely utilized for heating applications in residential, agricultural, and industries [2, 3]. However, this technique has a main drawback: the convection mechanism is weak in SAHs [4, 5]. This issue causes the thermal efficiency of SAHs to reduce significantly, and they were categorized as low-temperature heat sources

\*Corresponding Author Email: [hadi.farzan@bam.ac.ir](mailto:hadi.farzan@bam.ac.ir) (H. Farzan)

[6]. Hence, several methods, such as artificial roughness, have been developed and assessed to handle this problem [7, 8]. Perforations effectively improve turbulence and increase the convective heat transfer mechanism [9, 10]. The current study analyzes a novel SAH using a square perforated absorber plate to ameliorate the weak convection mechanism and improve thermal efficiency [11, 12].

Artificial roughness is an effective technique extensively analyzed and utilized in recent studies. This technique mainly emphasizes using baffled [13], finned [14, 15], and corrugated absorbers [16], simultaneously increasing friction factor and convection heat transfer coefficients [17, 18]. The perforation method is an applicable, robust method that can be served instead of the artificial roughness method; however, this method attracts little attention. Shetty et al. [19] studied a SAH utilizing a circular perforated absorber plate to improve thermal efficiency and assess how perforations affect the thermal efficiency of SAHs. This investigation illustrates that increasing the perforations' number and diameter enhances the thermal efficiency of SAHs significantly; however, the thermohydraulic efficiency may experience a marginal drop by further increasing these crucial parameters. Shetty et al. [20] conducted another investigation and developed a computational fluid dynamics (CFD) model for a perforated SAH to optimize the number and diameter of perforations. They proved that the perforated SAH's efficiency strongly depends on the perforations' diameter, while the highest thermal efficiency achieved by optimization is nearly 72.8%. Saravanan et al. [21] compared a SAH utilizing a C-shape finned perforated absorber plate with one using a smooth absorber in an experimental approach. Experimental runs were carried out in various Reynolds numbers and geometrical parameters. The acquired data showed that the perforated finned SAH has nearly 167% higher thermal efficiency than the SAH with a smooth, flat absorber. Arunkumar et al. [11] performed a numerical/experimental investigation to analyze a duct SAH with a perforated absorber considering different duct height ratios and holes' number and diameters. The acquired data illustrate that the perforation significantly increased the thermal and thermo-hydraulic efficiency of the perforated duct SAH, while the highest efficiency of 83% was achieved using a hole diameter of 5 cm and a duct height ratio of 0.667.

Hedau and Saini [22] developed a CFD model to assess the efficiency of a double-pass SAH with perforated artificial roughness. This study evaluated the SAH in various scenarios, including different Reynolds numbers and collector configurational parameters, and concluded that increasing the open area ratio and decreasing the relative height ratio improves the thermal efficiency of the perforated double-pass SAH. Farzan and Zaim [23] utilized the perforation method and porous materials simultaneously to increase the thermal

efficiency of double-pass solar heaters. Steel wools were used as porous mediums, and two scenarios were considered, including the porous perforated and non-porous perforated SAHs. They illustrated by using the porous medium increased the efficiency of the perforated SAH by nearly 15.3%. Eiamsa-Ard et al. [24] evaluated the heat transfer mechanism and thermal performance in a SAH using the perforated baffles. This study compared and analyzed two types of baffles: solid-transverse and square-wings baffles. The numerical results proved that the square-wing baffled SAH is more efficient than the solid-transverse SAH. Furthermore, they assessed the heat transfer rate in various wing positions to maximize thermal efficiency. Farzan and Zaim [25] combined a perforated metallic SAH with a pavement SAH to extend the operating period of SAH. Since the operating period of SAH is a function of incident solar energy and metallic SAH is unavailable when the solar intensity is absent. This strategy assists in saving

energy in pavement and prolongs the operating period of the combined SAH.

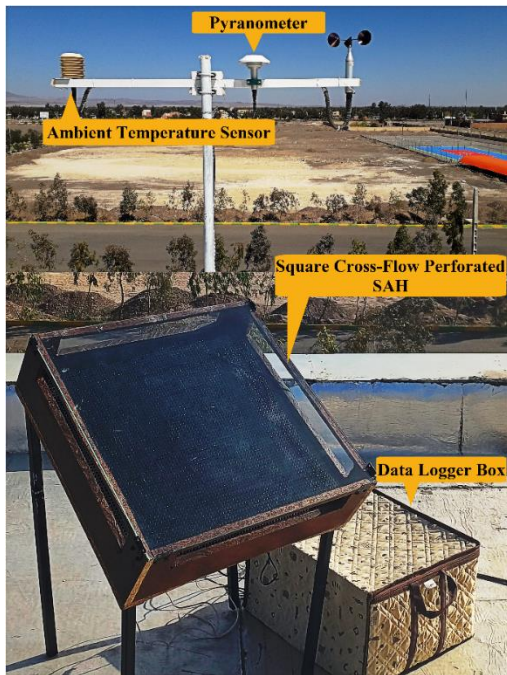
The late and recent studies focused on perforated SAHs mainly investigated the impacts of utilizing the perforated artificial roughness on the thermal performance of SAHs [11, 21, 22, 24]. However, using the perforated absorber is a practical approach that can improve the convective heat transfer rate. As discussed in the current literature review, using the perforated artificial roughness is an expensive, complicated technique and needs configurational and geometrical optimizations to obtain the highest performance. Furthermore, the perforated absorber plate is cheaper than the conventional or perforated artificial roughness. The current study introduces a novel cross-flow SAH type utilizing a perforated absorber. Combining the cross-flow pattern and perforation method boosts the convective heat transfer rate inside the SAH and consequently improves thermal performance. The other contribution of the current study is that the fabricated SAH uses a rectangular-shape configuration, which is a simple, cheap structure compared to other studies that employed circular-shape configurations to analyze perforated SAHs [19, 20].

The cross-flow pattern is a new airflow pattern, which is recently utilized in SAHs. This airflow pattern maximizes turbulence; high turbulence and higher heat exchange rate. The cross-flow pattern has been extensively utilized in various heat exchanger types to improve the convection mechanism. Since SAHs are a type of heat exchanger, this study provides this chance to examine the cross-flow airflow pattern in enhancing convection heat exchange in SAHs. Furthermore, using the perforation method assists the air to pass through the hot absorber plate, which has significantly enhanced the convection rate. Hence, increasing turbulence and perforation are techniques analyzed in the current study to improve the thermal performance of SAHs.

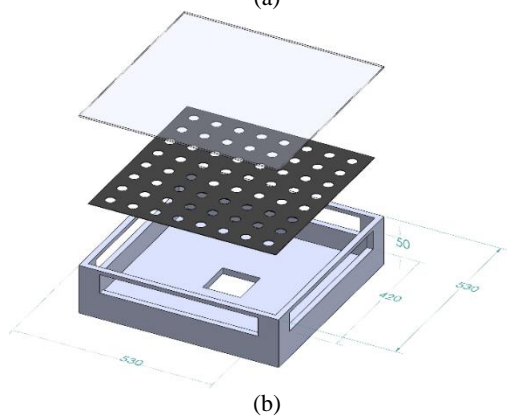
## METHODOLOGY

### Experimental setup

Figure 1 shows the cross-flow perforated SAH and presents the schematic draw of the experimental setup. The fabricated SAH has a medium-density fiberboard (MDF) box with a square perforated absorber plate of 0.2 m in length. This perforated absorber plate has 100 holes with a 2 mm diameter. These perforations were distributed homogenously on the heat absorber plate. Since the constructed SAH has a cross-flow configuration, it has four intake openings that the flowing air enters the SAH by passing through them. Each intake opening has a 0.02 m width and 0.18 m length. A commercial glass sheet with a 4 mm thickness placed 0.05 cm above the absorber protecting the perforated absorber plate.



(a)



(b)

**Figure 1.** (a) Experimental setup and (b) schematic of square cross-flow perforated SAH

A 10-Watt centrifugal fan was mounted at the bottom of the MDF box, which pulls the air to pass through the perforated absorber and exhausts it. Figure 2 shows the schematic of airstreams in the fabricated cross-flow perforated SAH. The fan speed was controlled by using a dimmer switch to produce desired airflow rates. The SAH was positioned at 30° facing south to maximize the incident solar energy.

### Experimental procedure and instrumentation

The experiments were performed in Bam, Iran (29.0985° N, 58.3375° E) at outdoor conditions. The experiments began at 9:00 A.M. and continued 24 hours until the next day for several consecutive days in April 2023 for  $m_{air} = 0.015$  kg/s and 0.03 kg/s. The weather conditions were sunny and stable during experiments to ensure the validity of the experimental method. Since experimental runs were carried out on consecutive days, ambient parameters slightly changed on these days during the experimental runs.

Several sensors monitored the transient dynamics of the constructed collector while the Rahgosha GX-800 datalogger recorded the measured data. Since weather conditions play a critical role in the dynamics of the constructed SAH, the ambient temperature and the solar intensity were measured using precise sensors, including Parto Negar TH202-485 and CMP3 Kipp & Zonen pyranometer. The absorber and outlet air temperatures are other crucial factors determining the dynamics of the cross-flow perforated SAH. These parameters were measured using NTC thermistors installed on the absorber plate and outlet opening.

The data acquired by these sensors contain errors due to instrumental, environmental, and procedural sources. Hence, precise and accurate experimental data are crucial to ensure the accuracy of the obtained results. Accuracy determines whether or not an instrument truly measures what it is aimed to measure, while uncertainty refers to the idea that all data have a range of expected values due to random errors. Kline [26] suggested a technique to

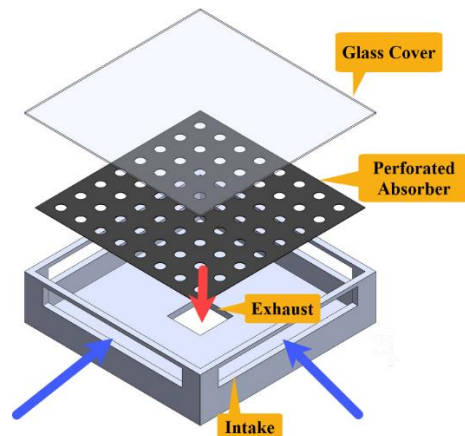


**Figure 2.** Flow-pattern in square cross-flow perforated SAH

calculate the standard uncertainty of the measured data as follows:

$$\frac{\omega_{\dot{m}_{air}}}{\dot{m}_{air}} = \left[ \left( \frac{\omega_{T_{air}}}{T_{air}} \right)^2 + \left( \frac{\omega_{v_{in}}}{v_{in}} \right)^2 + \left( \frac{\omega_{P_{air}}}{P_{air}} \right)^2 \right]^{\frac{1}{2}} \quad (1)$$

$$\frac{\omega_{Q_{useful}}}{Q_{useful}} = \left[ \left( \frac{\omega_{\dot{m}_{air}}}{\dot{m}_{air}} \right)^2 + \left( \frac{\omega_{\Delta T}}{\Delta T} \right)^2 \right]^{\frac{1}{2}} \quad (2)$$

$$\frac{\omega_{\eta}}{\eta} = \left[ \left( \frac{\omega_{\dot{m}_{air}}}{\dot{m}_{air}} \right)^2 + \left( \frac{\omega_{\Delta T}}{\Delta T} \right)^2 + \left( \frac{\omega_G}{G} \right)^2 \right]^{\frac{1}{2}} \quad (3)$$

here  $\omega_x$  is the uncertainties associated with the factor  $x$ . Table 1 shows the standard uncertainties of the critical parameters.

### ENERGY

Since numerous methods are suggested to compare and assess the efficiency of systems, energy analysis is a robust technique for this aim. The energy analysis is carried out based on first law of thermodynamics using inlet and outlet energy streams crossing the system's boundaries.

The perforated absorber is exposed to incident solar energy, and its temperature and energy content increase during diurnal hours. The air passes through the hot perforated absorber and gets heated; hence a portion of incident energy is transferred into the flowing air, and the remaining portion loses due to convective/radiant dissipations. To improve the efficiency of the SAH, it is required to increase the useful harnessed energy and decrease ambient heat losses. The energy analysis assists in comparing various techniques to achieve this aim and improve the efficiency of SAHs. The daily thermal efficiency of SAHs is defined as follows:

$$\eta_{I,Daily} = \frac{Q_{harnessed}}{Q_{incoming}} \quad (4)$$

**Table 1.** Accuracy and standard uncertainty of main factors

Factor	Accuracy	Standard Uncertainty
Measured Factors	Inlet & Outlet Temperature	±0.5 °C
	Ambient Temperature	±0.5 °C
	Solar Intensity	±10 W/m <sup>2</sup>
Calculated Factors	Air Mass Flow Rate	N.A.
	Harnessed Heat	±5.14%
	Thermal Efficiency	±3.25%

here  $Q_{harnessed}$  is the total useful harnessed energy by the SAH, and  $Q_{incoming}$  is the total energy hitting the absorber plate. The total useful harnessed energy and total incident energy are obtained as follows:

$$Q_{harnessed} = \int_0^{\Delta t} \dot{m}_{air} c_{p,air} (T_{air,out} - T_{air,in}) dt \quad (5)$$

$$Q_{incoming} = \int_0^{\Delta t} A_c G dt \quad (6)$$

here  $\dot{m}_{air}$  is the air mass flow rate, and  $A_c$  shows the collector surface area.  $G$  is the solar intensity, and  $c_p$  defines the air specific heat capacity.  $T_{air,in}$  and  $T_{air,out}$  denote the inlet and outlet air temperatures.

### RESULTS AND DISCUSSION

The present study assesses a novel cross-flow perforated SAH that utilizes the perforation technique and the cross-flow configuration to increase turbulence and convective rate. To achieve this goal, a cross-flow perforated SAH was fabricated and analyzed at outdoor conditions to precisely monitor the collector's dynamics and evaluate its thermal efficiency. Ambient conditions are critical factors significantly affecting the dynamics of the SAH. Figure 3 depicts the measured ambient conditions for 24 hours during the experiments. As shown in Figure 3, the solar intensity increases as experiments begin and experiences its maximum value, nearly 1100 W/m<sup>2</sup>, by 12:30. The solar intensity starts to reduce in the afternoon and approaches zero at 5:30 P.M.

The solar intensity defines the amount of incident energy; in other words, the higher the solar intensity, the higher the incident energy is. The high incident energy increases the absorber temperature or energy content, affecting the SAH's efficiency. The hotter the absorber, the higher the outlet temperature and, consequently, the higher the thermal efficiency. However, the hotter absorber temperature has high ambient heat dissipations, reducing the SAH's efficiency. Hence, it is required to improve the convection rate in the SAH by extracting more thermal energy.

The ambient temperature is nearly 17 °C at the beginning of the experiments in the morning and increases to nearly 22 °C at noon, then reduces continuously in the afternoon. The ambient temperature reaches 11 °C nearly one hour before sunrise, the coldest temperature during the day. The ambient temperature determines the inlet temperature; furthermore, it has a crucial impact on convective heat losses since the ambient temperature specifies the thermal potential difference or convective driving force.

Figure 4 represents the absorber temperature measured during the experiments. The absorber temperature quickly reacts to the incident solar radiation, and its temperature increases by increasing the solar

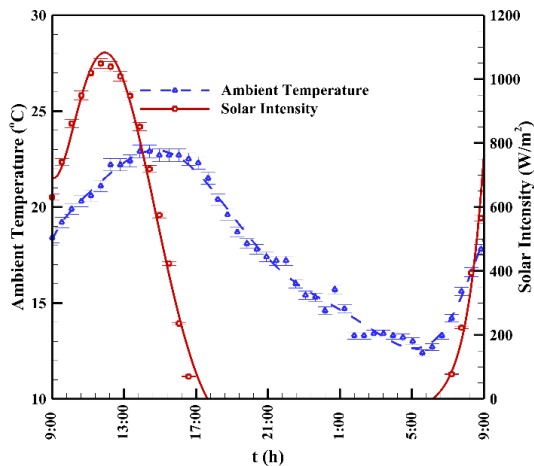


Figure 3. Measured ambient conditions

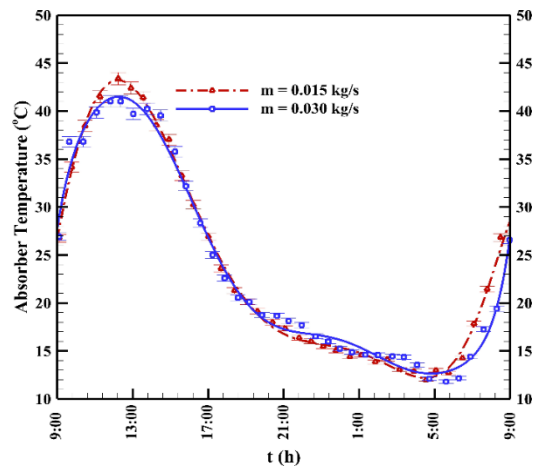


Figure 4. Measured absorber temperature

intensity. The absorber temperature is nearly 27 °C in the morning at 9:00 A.M., then increases and reaches to the maximum temperature of 44 °C and 41 °C for  $m_{air} = 0.015$  kg/s and 0.03 kg/s, respectively. The temperature profiles lay on top of each other in the afternoon, which means the collector's transient dynamics are close in the afternoon when the incident solar radiation is absent or insufficient. At night, the absorber temperature attains the ambient temperature and reduces by nearly 11 °C for both air flow rates ( $m_{air}$ ). This crucial issue reveals that the absorber temperature strongly depends on the incident solar radiation. Since steel has a low heat capacity, the absorber cannot store sufficient thermal energy during diurnal hours. Furthermore, the absorber sharply reacts to the ambient temperature at night due to the high heat conductivity of steel and high convection rate. These issues caused the absorber temperature profile to ascend and descend quickly by increasing and decreasing the incident solar energy.

Interestingly, the absorber temperature is slightly affected by  $m_{air}$ , and the absorber temperature profiles only have a small difference, nearly 3 °C, at their peak values. Indeed, using the perforations and cross-flow configuration provide a high convection rate and turbulence in the SAH. This issue causes that increasing the mass flow rate, which has the same effects (high convection rate and turbulence), does not significantly affect the dynamics of the SAH like conventional SAHs.

Figure 5 shows the measured outlet temperature during experimental runs. The measured outlet temperature depends on the inlet air temperature, convection rate, and absorber temperature. The absorber temperature shows the utmost potential temperature of the outlet temperature. Many investigations attempt to increase the convection rate and reduce the temperature difference between the hot absorber and outlet air temperatures. Interestingly, the maximum difference between the absorber and outlet temperatures reached nearly 6 °C and 7 °C for  $m_{air} = 0.015$  kg/s and 0.03 kg/s,

respectively. Furthermore, the temperature difference between the ambient and outlet temperatures is higher than that between the absorber and outlet temperatures. This crucial issue reveals a high convection rate in the SAH.

The outlet temperature has the same trend as the absorber temperature, or in other words, the outlet temperature increases by increasing the absorber temperature and vice versa. As shown in Figure 5, at the beginning of the morning and in the afternoon, the outlet temperature profiles lay on top of each other like the absorber temperature profiles. In the absence of incident solar energy, the outlet temperature reaches the ambient temperature by nearly 4:00P.M., and these temperatures have the same value at night. However, the outlet temperature sharply reacts to incident solar energy at the beginning of the morning for the next day and increases in a steep gradient.

Interestingly, the outlet temperature reaches slightly below the ambient temperature at night. Since the incident solar radiation is zero at night, the absorber

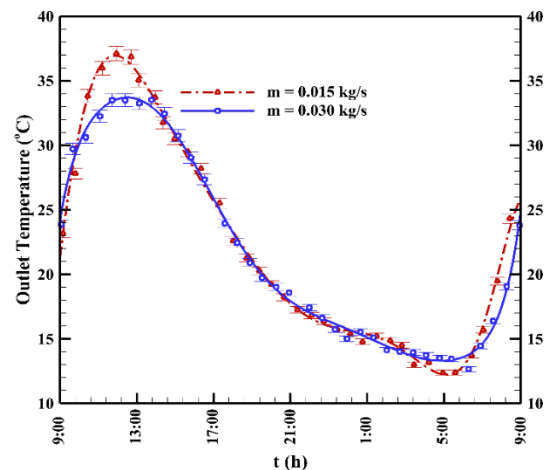


Figure 5. Measured outlet temperature



temperature exchanges radiant energy with the black sky and ambient environments. Hence the absorber temperature reaches slightly below the ambient temperature. This issue causes the air passing through the cold absorber to experience temperatures below the ambient temperature at night for a few hours.

Figure 6 shows the useful harnessed heat by the constructed SAH for each hour during the experiments. As seen in Figure 6, the harnessed thermal energy by the SAH increases in the morning until noon, then decreases in the afternoon by reducing the incident solar radiation. The peak values of the harnessed heat occur at periods when the outlet temperature attains its maximum value. The maximum values of the hourly harnessed heat for  $m_{air} = 0.015$  kg/s and 0.03 kg/s were nearly 220.8 kJ and 372.2 kJ, respectively. The obtained maximum values illustrate that the mass flow rate is doubled, but the maximum harnessed heat has increased by nearly 68.8%.

The harnessed heat has negative values at night for a couple of hours before sunrise, which reveals that the flowing air loses its heat content in some nighttime periods. It is required to note that the harnessed heat remains within a band of 10% around its peak values, or in other words, the harnessed energy varies in a range of  $340 \pm 30$  kJ and  $190 \pm 20$  kJ during 4 hours from 10:00A.M. to 2:00P.M. for both air flow rates,  $m_{air}$ . This issue proves that utilizing the perforations and cross-flow configuration provide a high convection rate in the SAH that the heat is sufficiently extracted from the hot absorber plate by the flowing air.

The harnessed energy has a steep gradient at sunset and sunrise, also seen in the outlet and absorber temperature profiles. Since the SAH has no heat storage system and the absorber has high thermal conductivity, these steep gradients occur when the incident solar energy significantly varies.

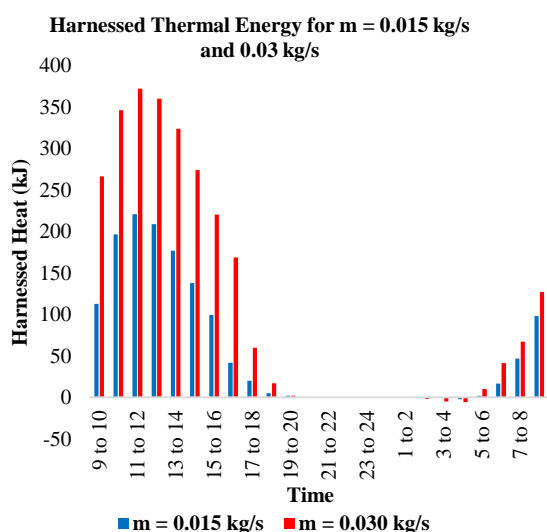


Figure 6. Calculated harnessed thermal energy

Table 2 summarized the daily thermal efficiency of the cross-flow perforated SAH. As shown in Table 2, the calculated efficiency for  $m_{air} = 0.015$  kg/s and 0.03 kg/s reached to 53.2% and 78.6%, respectively. Since various types of SAHs are available, a wide range of thermal efficiency has been reported for these SAHs. However, the daily thermal efficiency of nearly 78.6% is high, which illustrates that utilizing the perforations and cross-flow configuration are effective techniques, significantly improved the daily thermal efficiency.

Table 3 briefly compares perforated SAHs, different types of perforation methods, and obtained thermal efficiencies. This table illustrates that perforated absorbers are a suitable replacement for artificially roughened absorbers. Furthermore, Table 3 reports studies that assess various perforated SAHs. These SAH types have high thermal efficiency; however, they are expensive and technically complicated compared to the introduced square cross-flow perforated SAH. Hence, the square cross-flow perforated SAH are cheap, applicable, compact collectors with high thermal efficiency.

Table 2. Calculated daily thermal efficiency

Mass Flow Rate	Daily Thermal Efficiency	Useful Harnessed Energy
$m_{air} = 0.015$ kg/s	78.6%	2643 kJ
$m_{air} = 0.030$ kg/s	53.2%	1790 kJ

Table 3. Brief comparison between different perforated SAHs types

Reference	SAH Type	Thermal Efficiency
Shetty et al. [19, 20]	Circular cross-flow perforated SAH	72.8% to 75.55%
Farzan and Zaim [23]	Double-pass perforated SAH using porous materials	49.1% to 66.1%
Saravanan et al. [21]	SAH with staggered C-shape perforated finned absorber	68.8%
Farzan and Zaim [25]	Combined metallic/asphalt SAH using inclined perforated absorber	80%
Arunkumar et al. [11]	SAH with rectangular perforated duct inserts	83.01% to 87.06%
Current study	Square cross-flow perforated SAH	78.6%

## CONCLUSION

The present study introduced a novel square cross-flow perforated SAH and analyzed this collector at outdoor conditions to monitor its heat dynamics and thermal

performance. Using perforations and cross-flow configuration produces high turbulence that causes a high convection rate in the SAH. Since SAHs suffer from a weak heat convection mechanism and low thermal efficiency, producing high turbulence and heat exchange rates increases the thermal efficiency of SAHs. To examine the utilized thermal enhancement techniques, an experimental setup was fabricated and several sensors were employed to measure crucial parameters, including ambient factors, absorber, and outlet temperatures. The obtained results concluded that:

- At noon, the absorber temperature for  $m_{air} = 0.015\text{kg/s}$  and  $0.03\text{ kg/s}$  reached to the highest value of  $44\text{ }^{\circ}\text{C}$  and  $41\text{ }^{\circ}\text{C}$ , respectively. Interestingly, the maximum values of the measured outlet temperature were close in the scenarios considered.

- The outlet temperature reached to the maximum values of  $38\text{ }^{\circ}\text{C}$  and  $34\text{ }^{\circ}\text{C}$ , which is only  $6\text{ }^{\circ}\text{C}$  and  $7\text{ }^{\circ}\text{C}$  lower than the peak values of the absorber temperature for  $m_{air} = 0.015\text{ kg/s}$  and  $0.03\text{ kg/s}$ , respectively. This crucial issue revealed a high heat exchange rate in the SAH between the absorber and flowing air.

- The absorber and outlet temperature reacts quickly to the incident solar radiation and increases and decreases rapidly by increasing and decreasing the solar radiation. Indeed, the constructed SAH has no storage system. This issue caused the system to react quickly to the variation of the incident energy.

- The harnessed heat represents the same trend as the absorber and outlet temperatures at the beginning of the morning and in the afternoon. Furthermore, the harnessed thermal energy remains within a band of 10% around its peak values for 4 hours.

- In other words, providing a high heat exchange rate in the SAH causes the harnessed heat to vary between  $340 \pm 30\text{ kJ}$  and  $190 \pm 20\text{ kJ}$  during 4 hours from 10:00A.M. to 2:00P.M. for two considered air mass flow rates.

- The calculated efficiency of the cross-flow perforated SAH is nearly 53.2% and 78.6% for  $m_{air} = 0.015\text{ kg/s}$  and  $0.03\text{ kg/s}$ , which are high values compared to available SAHs types.

- In conclusion, the square cross-flow perforated SAH is cheap, applicable, and compact with high thermal efficiency. These specifications enhance this SAH type to have the potential to be utilized in wide heating applications.

For further studies, it is suggested that the square cross-flow perforated SAH is integrated with a heat storage unit to prolong its operating period and improve its thermal efficiency. Since this SAH provides a high heat exchange rate, utilizing an integrated heat storage unit can further increase its thermal efficiency.

## ACKNOWLEDGEMENT

The authors are thankful to the Higher Education Complex of Bam for their collaborative research.

## CONFLICT OF INTEREST

There is no conflict of interests.

## REFERENCES

1. Hayati, M., S. Ranjbar, M.R. Abdar, M. Molaei Nasab, S. Homayounmajd and M. Esmaeili Shayan, 2023. A Comparative Analysis of Solar Energy Strategies in Middle East with Rich Fossil Resources. *Iranian (Iranica) Journal of Energy & Environment*, 14(3), pp. 271-288. Doi:10.5829/ijee.2023.14.03.09
2. Goel, V., V. Hans, S. Singh, R. Kumar, S.K. Pathak, M. Singla, S. Bhattacharyya, E. Almatrafi, R. Gill and R. Saini, 2021. A Comprehensive Study on the Progressive Development and Applications of Solar Air Heaters. *Solar Energy*, 229, pp. 112-147. Doi: 10.1016/j.solener.2021.07.040
3. Ifrim, V.C., L.D. Milici, P. Atănăsoae, D. Irimia and R.D. Pentiu, 2022. Future Research Tendencies and Possibilities of Using Cogeneration Applications of Solar Air Heaters: A Bibliometric Analysis. *Energies*, 15(19), pp. 7114. Doi: 10.3390/en15197114
4. Khimsuriya, Y.D., D. Patel, Z. Said, H. Panchal, M.M. Jaber, L. Natrayan, V. Patel and A. El-Shafay, 2022. Artificially Roughened Solar Air Heating Technology-a Comprehensive Review. *Applied Thermal Engineering*, 118817. Doi: 10.1016/j.applthermaleng.2022.118817
5. Gandjalikhan Nassab, S. and M. Moein Addini, 2021. Performance Augmentation of Solar Air Heater for Space Heating Using a Flexible Flapping Guide Winglet. *Iranian (Iranica) Journal of Energy & Environment*, 12(2), pp. 161-172. Doi: 10.5829/ijee.2021.12.02.09
6. Arunkumar, H., K.V. Karanth and S. Kumar, 2020. Review on the Design Modifications of a Solar Air Heater for Improvement in the Thermal Performance. *Sustainable Energy Technologies and Assessments*, 39100685. Doi: 10.1016/j.seta.2020.100685
7. Sahu, M.K., V.K. Gorai and B.C. Saha, 2023. Applications of Extended Surfaces for Improvement in the Performance of Solar Air Heaters—a Detailed Systematic Review. *Environmental Science and Pollution Research*, pp. 1-19. Doi: 10.1007/s11356-023-26360-3
8. Yadav, A.S., A. Agrawal, A. Sharma, S. Sharma, R. Maithani and A. Kumar, 2022. Augmented Artificially Roughened Solar Air Heaters. *Materials Today: Proceedings*. Doi: 10.1016/j.matpr.2022.02.548
9. Singh, V.P., S. Jain and J. Gupta, 2022. Performance Assessment of Double-Pass Parallel Flow Solar Air Heater with Perforated Multi-V Ribs Roughness—Part B. *Experimental Heat Transfer*, 35(7), pp. 1059-1076. Doi: 10.1080/08916152.2021.2019147
10. Singh, V.P., S. Jain, A. Karn, G. Dwivedi, A. Kumar, S. Mishra, N.K. Sharma, M. Bajaj, H.M. Zawbaa and S. Kamel, 2022. Heat Transfer and Friction Factor Correlations Development for Double Pass Solar Air Heater Artificially Roughened with Perforated Multi-V Ribs. *Case Studies in Thermal Engineering*, 39102461. Doi: 10.1016/j.csite.2022.102461

11. Arunkumar, H., S. Kumar and K.V. Karanth, 2022. Performance Enhancement of a Solar Air Heater Using Rectangular Perforated Duct Inserts. *Thermal Science and Engineering Progress*, 34101404. Doi: 10.1016/j.tsep.2022.101404
12. Farzan, H., M. Mahmoudi and E. Hasan Zaim, 2023. Thermal Analysis of New Solar Air Heater with Inclined Perforated Absorber Plates: Experimental Study. *Iranian (Iranica) Journal of Energy & Environment*, 14(2), pp. 189-196. Doi: 10.5829/ijee.2023.14.02.11
13. Sethi, M., A.K. Singh, R. Tripathi, A. Kumar, S. Kumar, A. Thakur, B. Goel, T. Kashyap and V.K. Sharma, 2023. Influence of Distinct Baffles Type Turbulence Promoter on the Thermohydraulic Efficiency of Solar Air Heater: A Comprehensive Review. *Materials Today: Proceedings*, 72, pp. 1275-1283. Doi: 10.1016/j.matpr.2022.09.299
14. El-Said, E.M., M. Abou Al-Sood, E. Elsharkawy and G.B. Abdelaziz, 2022. Tubular Solar Air Heater Using Finned Semi-Cylindrical Absorber Plate with Swirl Flow: Experimental Investigation. *Solar Energy*, 236, pp. 879-897. Doi: 10.1016/j.solener.2022.03.054
15. Aouissi, Z., F. Chabane, M.-S. Teguaia, N. Belghar, N. Moumimi and A. Brima, 2022. Heat Exchange Optimization by Adding Baffles to Streaming Duct of Solar Air Collector. *Iranian (Iranica) Journal of Energy & Environment*, 13(4), pp. 349-353. Doi: 10.5829/ijee.2022.13.04.04
16. Kumar, P.G., V. Vigneswaran, K. Balaji, S. Vinothkumar, R. Prabhakaran, D. Sakthivadivel, M. Meikandan and S.C. Kim, 2022. Augmented V-Corrugated Absorber Plate Using Shot-Blasting for Solar Air Heater—Energy, Exergy, Economic, and Environmental (4e) Analysis. *Process Safety and Environmental Protection*, 165, pp. 514-531. Doi: 10.1016/j.psep.2022.07.036
17. Sahu, M.K., M. Kharub and M.M. Matheswaran, 2022. Nusselt Number and Friction Factor Correlation Development for Arc-Shape Apex Upstream Artificial Roughness in Solar Air Heater. *Environmental Science and Pollution Research*, 29(43), pp. 65025-65042. Doi: 10.1007/s11356-022-20222-0
18. Nanjundappa, M., 2021. Nusselt Number and Friction Factor Correlations for the Solar Air Heater Duct Furnished with Artificial Cube Shaped Roughness Elements on the Absorber Plate. *Heat and Mass Transfer*, 57(12), pp. 1997-2013. Doi: 10.1007/s00231-021-03067-0
19. Shetty, S.P., A. Paineni, M. Kande, N. Madhwesh, N.Y. Sharma and K.V. Karanth, 2020. Experimental Investigations on a Cross Flow Solar Air Heater Having Perforated Circular Absorber Plate for Thermal Performance Augmentation. *Solar Energy*, 197, pp.254-265. Doi: 10.1016/j.solener.2020.01.005
20. Shetty, S.P., N. Madhwesh and K.V. Karanth, 2021. Numerical Analysis of a Solar Air Heater with Circular Perforated Absorber Plate. *Solar Energy*, 215416-433. Doi: 10.1016/j.solener.2020.12.053
21. Saravanan, A., M. Murugan, M.S. Reddy, P. Ranjit, P. Elumalai, P. Kumar and S.R. Sree, 2021. Thermo-Hydraulic Performance of a Solar Air Heater with Staggered C-Shape Finned Absorber Plate. *International Journal of Thermal Sciences*, 168107068. Doi: 10.1016/j.ijthermalsci.2021.107068
22. Hedau, A. and R. Saini, 2023. Thermo-Hydraulic Performance of Double Pass Solar Air Heater Duct Having Semi-Circular Tubes and Perforated Blocks as Artificial Roughness. *Renewable Energy*, 205, pp.543-562. Doi: 10.1016/j.renene.2023.01.087
23. Farzan, H. and E.H. Zaim, 2023. Thermal Analysis of a New Double-Pass Solar Air Heater Using Perforated Absorber and Porous Materials: An Experimental Study. *Thermal Science and Engineering Progress*, 38101680. Doi: 10.1016/j.tsep.2023.101680
24. Eiamsa-Ard, S., A. Phila, M. Pimsarn, N. Maruyama and M. Hirota, 2023. Heat Transfer Mechanism and Thermal Performance of a Channel with Square-Wing Perforated Transverse Baffles Installed: Effect of Square-Wing Location. *Journal of Thermal Analysis and Calorimetry*, pp. 1-15. Doi: 10.1007/s10973-022-11937-w
25. Farzan, H. and E.H. Zaim, 2023. Study on Thermal Performance of a New Combined Perforated Metallic/Asphalt Solar Air Heater for Heating Applications: An Experimental Study. *Solar Energy*, 249, pp. 485-494. Doi: 10.1016/j.solener.2022.12.008
26. Kline, S.J., 1963. Describing Uncertainties in Single-Sample Experiments. *Mechanical Engineering*, 75, pp. 3-8.

#### COPYRIGHTS

©2021 The author(s). This is an open access article distributed under the terms of the Creative Commons Attribution (CC BY 4.0), which permits unrestricted use, distribution, and reproduction in any medium, as long as the original authors and source are cited. No permission is required from the authors or the publishers.





## Persian Abstract

## چکیده

مطالعه حاضر نوع جدید از گرمکن‌های هوایی مشبک با جریان عرضی را معرفی و بررسی می‌نماید. از آنجایی که مکانیزم انتقال حرارت جابجایی در گرمکن‌های خورشیدی هوایی ضعیف و نامناسب است، تاکنون روش‌های متنوعی برای بهبود انتقال حرارت جابجایی و متعاقباً افزایش راندمان حرارتی در این دسته از کلکتورهای خورشیدی پیشنهاد شده است. از آنجایی که استفاده از صفحات جاذب مشبک و الگوی جریان عرضی اغتشاش و آشفتنگی مناسبی در جریان هوا ایجاد می‌نماید، این روش‌ها سبب بهبود انتقال حرارت جابجایی و در نتیجه افزایش راندمان حرارتی در گرمکن‌های هوایی می‌گردند. برای آزمودن این رویکردها در افزایش راندمان حرارتی، یک گرمکن هوایی با صفحه جاذب مشبک و جریان عرضی ساخته و در شرایط محیطی در دبی‌های جرمی  $0.15 \text{ kg/s}$  و  $0.3 \text{ kg/s}$  آزمایش شده است. در حین آزمایش حسگرهای متعددی برای نظارت و ثبت رفتار دینامیکی گرمکن و شرایط محیطی استفاده شده است. نتایج بدست آمده نشان می‌دهد دمای هوای خروجی به بیشینه مقادیر  $38^\circ\text{C}$  و  $34^\circ\text{C}$  برای دبی‌های جرمی در نظر گرفته شده می‌رسد، در حالیکه این مقادیر تنها  $6^\circ\text{C}$  و  $7^\circ\text{C}$  از بیشینه مقادیر دمای صفحه جاذب کمتر هستند. از آنجا که دمای صفحه جاذب و هوای خروجی به یکدیگر نزدیک هستند، این مهم نشان‌دهنده نرخ انتقال حرارت جابجایی بالا به دلیل اغتشاش بالای جریان هوا در این گرمکن هوایی است. مکانیزم انتقال حرارت جابجایی قوی در گرمکن مورد بررسی سبب افزایش راندمان حرارتی روزانه و رسیدن این راندمان به عدد مناسب  $0.78/6$  برای دبی جرمی  $0.3 \text{ kg/s}$  می‌شود. در نتیجه، گرمکن خورشیدی هوایی با صفحه جاذب مشبک و جریان عرضی، گرمکنی با ساختاری ارزان، کاربردی و فشرده است که راندمان حرارتی بالایی را تضمین می‌کند.